# Robust PID Controller of BLDC Motor via State Feedback Design

Petru Dobra

Abstract— **The $PID$ controller is most commonly used for industrial applications. I consider the speed control which are encountered in practical applications, and I propose a state space parametrization which allows to convert $PID$ controller synthesis into an $LMI$ optimization problem. The paper reexamines the standard nested two loop controller structure for a permanent magnet brushless $DC$ motor in speed servo applications. An analysis of a generic example demonstrates that the robust synthesis, via $LMI$ optimization, offers noticeable improvements in performance especially in cases of (relatively large) model uncertainties. The proposed technique guarantees uniform exponential stability of the closed loop system, a desired rate of convergence, and $H^\infty$ norm bound.**

Keywords— $PID$, **Robust Control,** $LMI$, $BLDC$ **Motor, State Feedback Control**

## I. Introduction

TWO loop control structures are commonly used in motor drives, in speed control applications. This structure is widely perceived as very satisfactory, both from a control standpoint and from an apparatus protection point of view [6], [7]. The purpose of this paper is to quantify the sub-optimal $PID$ controller, nested in two loop control design algorithm for a permanent magnet brushless $DC$ ($BLDC$) motor in speed servo applications with respect to robustness of the system uncertainties. Specifically, we will focus on the case of an uncertain moment of inertia. Our analysis and design tools will be the Linear Matrix Inequality ($LMI$) based methods, as developed in [2], [10]. These methods are applicable to any motor and uncertainty type and are extendable to positioning problems as well.

As can be expected, our numerical experiments suggest that robust design procedures, such as the $LMI$ method, offer potentially significant improvements in robust performance, in cases of model uncertainties (see [8]). Yet in low comparable cases, the $LMI$ design method gives truly satisfactory dynamical response.

The paper reexamines the standard nested two loop controller structure for a permanent magnet $BLDC$ motor in speed servo applications. A robust synthesis, via Linear Matrix Inequalities ($LMI$) design, of a generic example demonstrates that robust design offers noticeable improvements in performance especially in cases of relatively large model uncertainties.

## II. Mathematical Model of the $BLDC$

The $Y$-connected, 3-phase motor with a 4-pole permanent magnetic rotor is driven by a $PWM$ inverter (see Fig. 1). The rotor position, which determines the switching sequence of the $MOSFET$ transistors, is detected by means of 3 Hall sensors mounted on the stator. The switching scheme implemented in the inverter logic is well-known (see e.g. [5], [9], [12]).

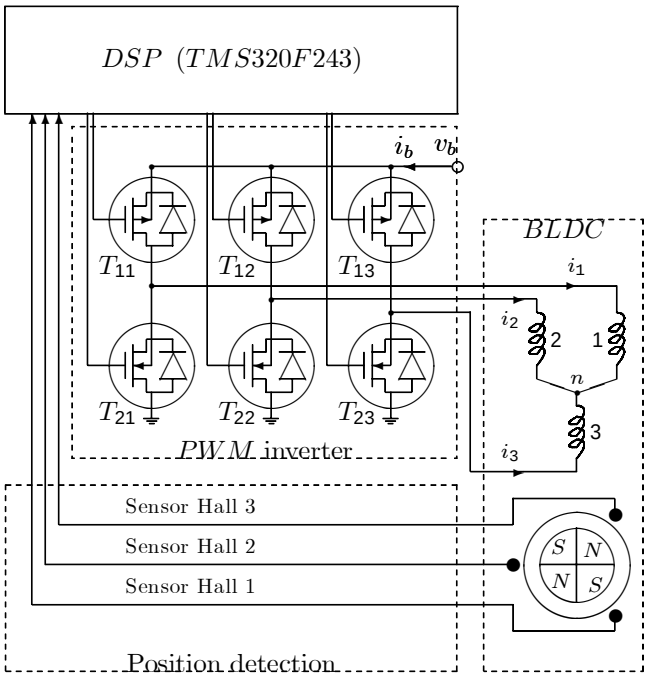


Fig. 1. $PWM$ inverter connected to the $BLDC$ motor

The mathematical model of the motor can be divided in two subsystems: an electrical and a mechanical model.

### A. Electrical Subsystem

Motor speed is controlled by adjusting the input voltage of the stator coils. For that purpose the $PWM$ rate is modulated on the active (conducting) transistor of the upper transistor row. The mathematical model of one coil (e.g. coil no. 1) can be derived from Fig. 2

$$v_1 - v_n = R_1 i_1 + L_1 \frac{di_1}{dt} + e_1.$$

The trapezoidal back-$emf$ of phase 1 is

$$e_1 = K_{e_1} \omega(t),$$

where $\omega(t)$ is the angular velocity of the rotor and $K_{e_1}$ the back-$emf$ constant. $v_1$ denotes the phase voltage with respect to reference potential and $v_n$ is the voltage at the star point (see [5]). Hence for all three phases the following

P. Dobra is with the Systems Theory Laboratory, Technical University of Cluj (TUC), Cluj RO-3400, ROMANIA. E-mail: dobra@aut.utcluj.ro.

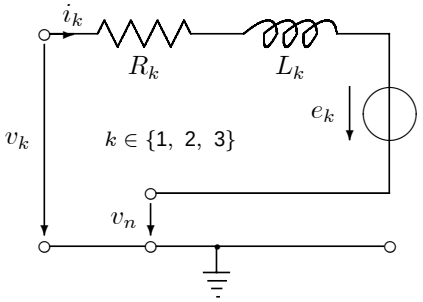


Fig. 2. Single phase equivalent circuit

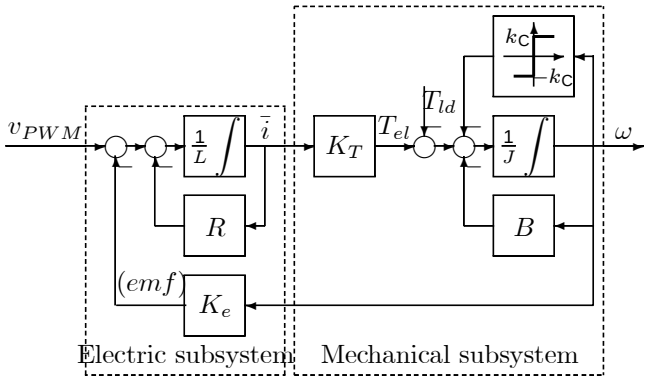


Fig. 3. Block diagram of the $BLDC$ motor model

system of equations holds

$$\begin{pmatrix} v_1 - v_n \\ v_2 - v_n \\ v_3 - v_n \end{pmatrix} = \begin{pmatrix} R_1 & 0 & 0 \\ 0 & R_2 & 0 \\ 0 & 0 & R_3 \end{pmatrix} \begin{pmatrix} i_1 \\ i_2 \\ i_3 \end{pmatrix} + + \begin{pmatrix} L_1 & 0 & 0 \\ 0 & L_2 & 0 \\ 0 & 0 & L_3 \end{pmatrix} \begin{pmatrix} \frac{di_1}{dt} \\ \frac{di_2}{dt} \\ \frac{di_3}{dt} \end{pmatrix} + \begin{pmatrix} K_{e_1} \\ K_{e_2} \\ K_{e_3} \end{pmatrix} \omega. \quad (1)$$

Usually, the star point cannot be accessed, so the respective voltage is unknown. As one of the coils is always open, the equation becomes simpler and one can eliminate $v_n$ in (1). Provided that coils 1 and 2 are conducting, the conditions $v_1 = v_{PWM}$, $v_2 = 0$, $i_2 = -i_1$ and $i_3 = 0$, are substituted in the equation (1), thus resulting in

$$v_{PWM} = (R_1 + R_2)\, i_1 + (L_1 + L_2)\, \frac{di_1}{dt} + + (K_{e_1} + K_{e_2})\, \omega(t). \quad (2)$$

The term $v_{PWM} = u \cdot v_b$ denotes the $PWM$ modulated supply voltage of the transistors, with $u \in [0, 1]$. Equivalent equations can be derived for 5 other cases (see [5]). To provide a reasonably inexpensive solution, and avoiding measurement of all 3-phase currents and voltages, only the input current of the 6-phase full bridge circuit $i_b$ and the supply voltage $v_b$ are measured. The average phase current $\bar{i}$ can be derived from the bridge current by considering the power balance

$$v_b \cdot i_b(t) = v_{PWM} \cdot \bar{i}(t) = u \cdot v_b \cdot \bar{i}(t).$$

Hence

$$\bar{i}(t) = \frac{i_b(t)}{u}.$$

Using this property and forming the mean value of equation (2) we get

$$v_{PWM} = \frac{2}{3}(R_1 + R_2 + R_3)\, \bar{i}(t) + \frac{2}{3}(L_1 + L_2 + L_3) \times \times \frac{d\bar{i}(t)}{dt} + \frac{2}{3}(K_{e_1} + K_{e_2} + K_{e_3})\, \omega(t).$$

Substituting finally $2/3 \times (R_1 + R_2 + R_3)$ by $R$ and $2/3 \times (K_{e_1} + K_{e_2} + K_{e_3})$, by $K_e$ leads to

$$v_{PWM} = R\bar{i}(t) + L\frac{d\bar{i}(t)}{dt} + K_e \omega(t). \quad (3)$$

## B. Mechanical Subsystem

After modelling the electrical subsystem of the actuator, the equations of the mechanical part will be given. Rotor torque results from the magnetic field caused by currents of the stator coil. This torque is proportional to the magnetic flux linkage and the average phase current. Hence

$$T_{el} = K_T \bar{i}(t),$$

with $K_T$ denoting the torque constant. For an ideal square wave motor (see [5]) it is equal to back-$emf$ constant $K_e$. The equation for the mechanical subsystem can be derived from the torque balance

$$T_{el} = T_{ld} + J\frac{d\omega}{dt} + T_{losses}, \quad (4)$$

where $T_{ld}$ is the load torque, $J$ denotes the inertia of the rotor and the losses ($T_{losses}$) result from friction. The mechanical losses can be split up into Coulomb friction $k_C \cdot sign(\omega(t))$ and viscose friction $B \cdot \omega(t)$. Thus, (5) finally yields

$$K_T \bar{i}(t) = T_{ld} + J\frac{d\omega}{dt} + B\omega + k_C \cdot \mathrm{sign}(\omega(t)), \quad (5)$$

Hence, the mathematical model of the $BLDC$ motor can be summarized by (3) and (5). The resulting model is depicted in Fig. 3. One can easily notice that it is similar to the model of the classical $DC$ motor.

## III. Conventional Controller

A simplified model of a $BLDC$ motor is presented in Fig. 3. It is assumed that the measurements of the motor speed $\omega$ and the armature current $i_a$ are available and that the control input is the voltage reference signal $u_c$, see Fig. 4. A $PI$ controller:

$$K_{PI}^{i_a}(s) = K_p^{i_a} + K_i^{i_a}\frac{1}{s}, \quad (6)$$

for the current loop is designed in the first step. Here we ignore the back $emf$, $E_a(s) = k_e \Omega(s)$, assuming that the current loop response dynamics is much faster. With this assumption, the closed loop current transfer function is:

$$G_{cl}^{i_a} \simeq \frac{K_p^{i_a} K_{PWM} s + K_i^{i_a} K_{PWM}}{Ls^2 + \left(K_p^{i_a} K_{PWM} + R\right) s + K_i^{i_a} K_{PWM}}. \quad (7)$$

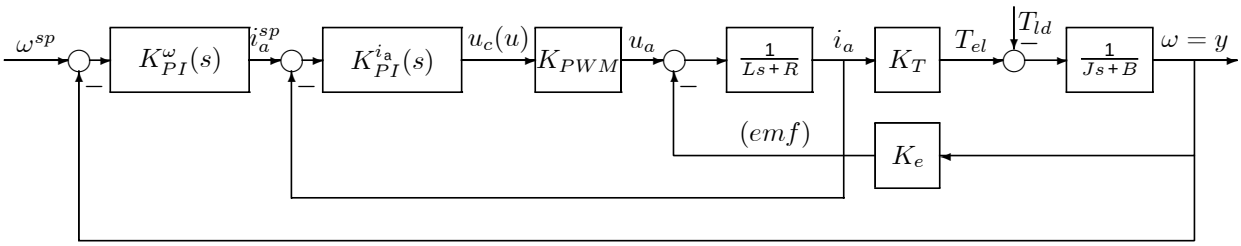


Fig. 4. Block diagram of the conventional nested $BLDC$ motor control structure

We also ignore the relatively small effects of $Ri_a$ on $\frac{d}{dt}T_e$ $\left(T_e = \frac{L}{R}\right)$. Under this assumption, the closed loop current transfer function is:

$$G^{i_a}_{cl} \simeq \frac{K^{i_a}_p K_{PWM} s + K^{i_a}_i K_{PWM}}{Ls^2 + K^{i_a}_p K_{PWM} s + K^{i_a}_i K_{PWM}}. \qquad (8)$$

We select the natural frequency $f^{i_a}_n = \frac{\omega^{i_a}_n}{2\pi}$ to be one tenth of the $PWM$ switching frequency $f_{PWM}$ (to ensure the validity of a linear approximation) and the damping $\zeta^{i_a} = 1$. The coefficients $K^{i_a}_p$ and $K^{i_a}_i$ are then derived from the equations:

$$\frac{K^{i_a}_i K_{PWM}}{L} = \left(\omega^{i_a}_n\right)^2, \quad \frac{K^{i_a}_p K_{PWM}}{L} = 2\zeta^{i_a}\omega^{i_a}_n. \qquad (9)$$

The design of the $PI$ speed controller:

$$K^{\omega}_{PI}(s) = K^{\omega}_p + K^{\omega}_i \frac{1}{s}, \qquad (10)$$

in the second step, a similar procedure is the following: the friction effects are neglected and the much faster current loop is approximated by the identity. The latter is justified by the selection of the speed closed loop natural frequency to be one tenth of that of the current loop. Under these assumptions, the closed loop angular speed transfer function is

$$G^{\omega}_{cl} \simeq \frac{K^{\omega}_p K_T s + K^{\omega}_i K_T}{Js^2 + K^{\omega}_p K_T s + K^{\omega}_i K_T}. \qquad (11)$$

Again a damping $\zeta^{\omega} = 1$ is fixed. The coefficients $K^{\omega}_p$ and $K^{\omega}_i$ are then derived from the equations:

$$\frac{K^{\omega}_i K_T}{J} = \left(\omega^{\omega}_n\right)^2, \quad \frac{K^{\omega}_p K_T}{J} = 2\zeta^{\omega}\omega^{\omega}_n. \qquad (12)$$

For our example we calculated the following data $\omega^{i_a}_n = 0.942 \times 10^3 \ \frac{rad}{\mathsf{sec}}$, $\omega^{\omega}_n = 0.942 \times 10^2 \ \frac{rad}{\mathsf{sec}}$, $K^{i_a}_p = 0.2873$, $K^{i_a}_i = 135.3230$, $K^{\omega}_p = 0.7345$, $K^{\omega}_i = 34.5971$.
Closed loop time responses are computed and depicted in Fig. 5, when the load inertia varies from 100% to 200% of its nominal value. We assume a constant load torque of $T_{ld} = 0.4 \ [N.m]$ and require a velocity (angular speed) of $\omega^{sp} = 1500 \ [rpm] = 50\pi \ \left[\frac{rad}{\mathsf{sec}}\right]$. We assume a constant load torque of $T_{ld} = 0.4 \ [N.m]$ and require a velocity (angular speed) of $\omega^{sp} = 1500 \ [rpm] = 50\pi \ \left[\frac{rad}{\mathsf{sec}}\right]$.

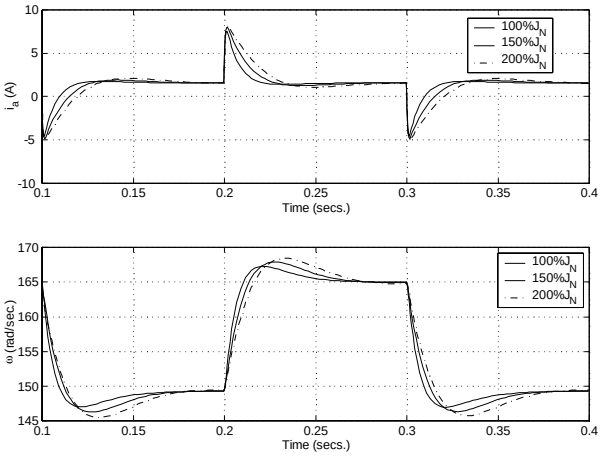


Fig. 5. Conventional design: closed loop time response of angular speed $(\omega)$ and current $(i_a)$, when load inertia varies from 100% to 200% of the nominal

## IV. $LMI$ Controller

Performance specifications (see [3]) for reference tracking and load rejection were based on the performance that was achieved in conventional design. The first step in the design procedure is to specify a generalized plant transfer matrix. The generalized plant $G$ comprises the model of the original system and the various weighting functions that represent performance specifications. Plant uncertainty is represented by an unspecified block $\Delta$ with a known $H^{\infty}$ norm bound, interacting with $G$ via disturbances signals $(\mathsf{w} \in \mathbb{R}^{n_w})$ and controlled signals that are to be regulated $(\mathsf{z} \in \mathbb{R}^{n_z})$. The generalized plant is driven by an the exogenous multivariable inputs $w$, including disturbances, sensor noise and the tracking reference. A controlled outputs $z$, represents tracking errors, actuating commands and outputs that can be measured. The closed loop mapping $T_{zw} : w \rightarrow z$ is required to be contractive. A stabilizing feedback controller, $K$, to be designed, will use the measured signal $y$ and produces the control input $u$.
A speed loop robust $PID$ controller

$$K_{PID}(s) = k_p + k_i \frac{1}{s} + k_d s \qquad (13)$$

comply with a:
(a) closed loop robust stability for rotor inertia $J$ varying from 100% to 200%;
(b) reasonable speed tracking performance;

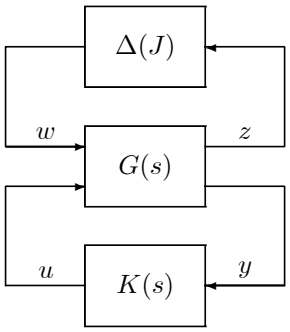


Fig. 6. Linear Fractional Reprezentation for uncertain nonlinear systems

(c) bounding of the command input $u_c$;
(d) current limiting $i_a$.

The $LMI$-based controller design will be designed in three steps: first, augmented the system by a Linear Fractional Representation ($LFR$); then, deducing of Linear Matrix Inequalities ($LMI'$s) that ensure the above specifications; finally, is showing of the results by numerical simulation.

### A. Construction of the $LFR$

The $LFR$ model can be constructed systematically, starting by the systems dynamic equations [1], [11]. It results in a model like the form depicted in Fig. 6, where $G(s)$ represents the nominal linear time-invariant system [4], [10]. The matrix $\Delta(J)$ contains rotor inertia uncertainties and is connected to the nominal system via input $w$ and output $z$. It can be written

$$\frac{dx}{dt} = \begin{pmatrix} -\frac{R_a}{L_a} & -\frac{K_e}{L_a} & 0 \\ \frac{K_T}{J_N} & -\frac{B}{J_N} & 0 \\ 0 & -1 & 0 \end{pmatrix} x + \\ + \begin{pmatrix} 0 \\ -\frac{1}{J_N} \\ 0 \end{pmatrix} w + \begin{pmatrix} \frac{K_{PWM}}{L_a} \\ 0 \\ 0 \end{pmatrix} u, \tag{14}$$

$$z = \begin{pmatrix} K_T & -B & 0 \end{pmatrix} x + \begin{pmatrix} -\frac{1}{J_N} \end{pmatrix} w, \tag{15}$$

$$u = \vartheta^{sp} - K_x x, \qquad w = \delta_J z, \quad |\delta_J| \le 1, \tag{16}$$

$$y = \begin{pmatrix} 0 & 1 & 0 \end{pmatrix} x, \tag{17}$$

where $J_N$ is the rotor inertia nominal value and $\delta_J$ represents the rotor inertia uncertainty such that $J = J_N(1+\delta_J)$, $x \in \mathbb{R}^{3\times 3}$ is the state

$$x = \begin{pmatrix} i_a, & \omega, & \int \omega \end{pmatrix}^T, \tag{18}$$

and

$$K_x = \begin{pmatrix} k_d \frac{K_T}{J}, & k_p - k_d \frac{B}{J}, & -k_i \end{pmatrix}. \tag{19}$$

### B. $LMI$ Conditions

We can readily normalize the system above so that it can be written as [11]:

$$\begin{pmatrix} \frac{dx}{dt} \\ z \\ y \end{pmatrix} = \begin{pmatrix} A & B_w & B_u \\ C_z & D_{zw} & D_{zu} \\ C_y & D_{yw} & D_{yu} \end{pmatrix} \begin{pmatrix} x \\ w \\ u \end{pmatrix}. \tag{20}$$

As can be seen in [2], [10], it is possible to formulate the synthesis conditions that ensure specifications $(a) \div (d)$, as defined previously, in a set of $LMI$ constraints. The $LMI$ condition that ensures a closed-loop robust $\alpha$-stability (every trajectory decays to zero at rate $\alpha$, that is $\lim_{t\to\infty} e^{\alpha t} x(t) = 0$) is equivalent to $\exists Q > 0,\ T > 0$ and $Y = K_x Q$ such that:

$$\left( \begin{array}{c|c} AQ + QA^T + B_u Y + Y^T B_u^T + 2\alpha Q & \cdots \\ \hline TB_w^T + C_z Q + D_{yu} Y & \cdots \end{array} \right. \\ \left. \begin{array}{c|c} \cdots & (2.1)^T \\ \hline \cdots & TD_{zw} + D_{zw}^T T - 2T \end{array} \right) < 0. \tag{21}$$

The $LMI$ condition that ensures a bound $u_{\max}$ on the command input $u(t)$ for every initial condition $x_0$ in the ellipsoid

$$\mathcal{E}_{\mathcal{Q}} = \left\{ \mathrm{x} \,\middle|\, \mathrm{x}^{\mathcal{T}} \mathcal{Q} \mathrm{x} \le \infty \right\}$$

is:

$$\left( \begin{array}{c|c} u_{\max}^2 I & Y \\ \hline Y^T & Q \end{array} \right) \le 0. \tag{22}$$

For every initial conditions that belong to the ellipsoid $\mathcal{E}_{\mathcal{Q}}$, some bounds $z_{\max}^i$, $i = \overline{1,\ n_z}$, can also be ensured for outputs $z_i = C_z^i \mathrm{x}$ with $LMI$ constraints:

$$\left(z_{\max}^i\right)^2 - C_z^i Q \left(C_z^i\right)^T \ge 0, \quad z_{\max}^i, i = \overline{1,\ n_z}. \tag{23}$$

### C. Simulation

The numerical results are obtained with the $MATLAB$. We synthesized a controller that ensures speed reference tracking for $\pm 5\%-$variations from its nominal value. It is assumed a constant load torque of $T_{ld} = 0.4\ [N.m]$ and it is required a velocity (angular speed) of $\omega^{sp} = 1500\ [rpm] = 50\pi\ \left[\frac{rad}{\mathrm{sec}}\right]$. This design provide the robustness of the closed-loop system with respect to rotor inertia uncertainties and so that the saturation bounds for current ($i_a \le i_a^{\max} = 10\ [A]$) and voltage ($u_c \le u_c^{\max} = 5\ [V]$) are not exceeded.

It is imposed a strong decay-rate by setting $\alpha = 72$ and it is found the controller $k_p = 1.7618$, $k_i = 594.5767$, $k_d = 1.4363e-3$. We plot in Fig. 7 responses of the closed loop system of angular speed ($\omega$) and current ($i_a$) when the load inertia varies from 100% to 200% of its nominal value.

## V. Conclusions

In this paper is to quantify the sub-optimal $PID$ controller, nested in two loop control design algorithm for a $BLDC$ motor in speed control applications with respect to robustness of the system uncertainties. A robust $PID$ controller is obtained by means of the solution of an $LMI$ feasibility problem. The numerical results confirm the validity of the proposed method in case of speed control and are extendable to positioning problems.

The synthesis of the $PID$ gains is converted into a static state-feedback controller synthesis on auxiliary system with parameter uncertainties. The controller presented (via $LMI's$) shows excellent robustness characteristic. This work demonstrates that state-feedback robust controller via $LMI's$ is very efficient and flexible in practical problems.

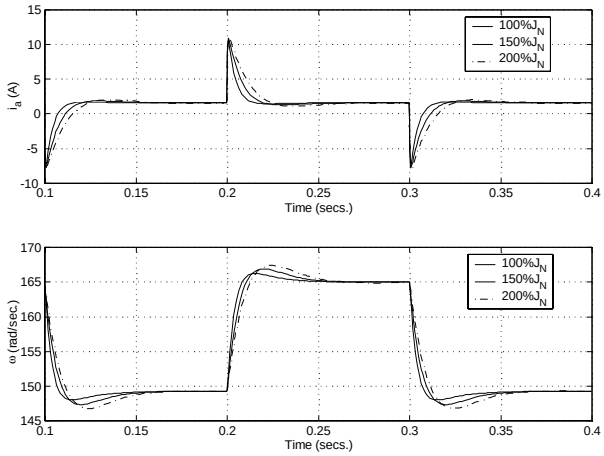


Fig. 7. *LMI* based design: closed loop time response of angular position ($\vartheta$), angular speed ($\omega$) and current ($i_a$), when load inertia varies from 100% to 200% of the nominal

## REFERENCES


[1] S. Battacharyya, H. Chapellat, and L. Keel, Robust Control. The Parametric Approach, Prentice Hall, New Jersey, 1995.

[2] S. Boyd, L. ElGhaoui, E. Feron, and V. Balakrishnan, Linear Matrix Inequalities in System and Control Theory, Vol. 15 of Studies in Applied Mathematics (SIAM), Philadelphia, PA, 1994.

[3] G. F. Franklin, J. D. Powell, and M. L. Workman, Digital Control of Dynamic Systems, Addison-Wesley, 1990.

[4] P. Gahinet, "Explicit controller formulas for LMI-based $H_\infty$ synthesis", Automatica, **32(7)**, 1007–1014, 1996.

[5] Hendershot, J.R., T. Miller, Design of Brushless Permanent-Magnet Motors, Magna Physics and Clarendon, Oxford, 1994.

[6] W. Leonard, "High performance microcomputer control of electrical drives". In C. Leodes (editor), Control and Dynamic Systems - Analysis and Control System Techniques for Electric Power Systems, Vol. 43, Academic Press, 1991.

[7] W. Leonard, Control of Electric Drives, Springer Verlag, London, 1985.

[8] M. Mattei, "Robust multivariabile PID control for linear parameter varying systems", Automatica, **37(12)**, 1997–2003, 2001.

[9] K. Oshio, T. Matsuo, H. Suemitsu, and K. Nakano, "Japan Fuzzy Adaptive Position Control of Blushless *DC* motors with Spiral Vector", Asian Control Conference, 9/25/2002.

[10] C. Scherer, P. Gahinet, M. Chilali, "Multiobjective output-feedback control via *LMI* optimization", IEEE Trans. on Automatic Control, AC-42(7), 896-911, 1997.

[11] K. Zhou, J. Doyle, and K. Glover, Robust and Optimal Control. Prentice Hall, New Jersey, 1996.

[12] ***** TMS320C/F241,C242,F243 DSP Controllers, Reference Guide (SPRU276), Texas Instruments, 1997.